Delivery of liposome encapsulated *temozolomide* to brain tumour: Understanding the drug transport for optimisation

Wenbo Zhan*

Department of Mechanical Engineering, Imperial College London, South Kensington Campus, London, United Kingdom

ARTICLE INFO

ABSTRACT

Temozolomide presents significant anticancer activities in preclinical trials. However, its clinical applications suffer from serious side effects owing to the high concentration in blood and normal tissues. In this study, mathematical modelling is applied to simulate the liposome-mediated delivery of *temozolomide* under different conditions in a 3-D realistic brain tumour model reconstructed from MR images. Delivery outcomes are evaluated by the bioavailability of free *temozolomide* across time. As compared to the oral and intravenous administration of free *temozolomide*, liposome-mediated delivery can successfully improve the drug accumulation in tumour while reducing the drug exposure in blood and normal tissue. Results show that the delivery is less sensitive to the duration of intravenous infusion but highly dependent on the liposome properties. The treatment can be improved by either enhancing the liposome transvascular permeability or using the liposomes with high extracellular release rates. Intravascular release can only increase the risk of adverse effects rather than improving the drug bioavailability in tumour. Results obtained in this study could be applied for optimising the treatment using liposome encapsulated *temozolomide*.

1. Introduction

Malignant glioma is one of the most aggressive and invasive diseases in clinic because of the high mortality rate (Mangiola et al., 2010). Despite of surgery followed by radiotherapy and chemotherapy, glioma could invariably recur and henceforth lead to rapid death (Xue et al., 2017). Blood-brain barrier (BBB) is the main obstacle in routine chemotherapy as it can successfully block the majority of drugs within the blood circulatory system and hence retard the drug accumulation in the tumour.

As an alkylating agent belonging to the imidazotetrazine series, *temozolomide* presents broad-spectrum anticancer activities with ubiquitous distribution in all the tissues (Friedman et al., 2000). It is favoured for brain tumour therapy due to the effectiveness of crossing the BBB (Pineda et al., 2017). However, the clinical applications are limited by several adverse effects owing to the high concentrations in blood and various normal tissues (Hanna et al., 2018). Liposomes have been developed for targeted treatment in which the encapsulated drugs are designed to be released in the lesion in a controllable manner. Although the feasibility of liposome-mediated delivery of *temozolomide* has been reported in preclinical studies (Huang et al., 2008; Gao et al., 2015),

this delivery system can be further optimised from the aspect of drug transport to improve the treatment efficacy.

Mathematical modelling has become a promising approach to investigate drug delivery due to the advantage for examining the multiple biophysical and physicochemical processes individually or in an integrated manner. The modelling framework was firstly established to study the transport of macromolecular drugs (Baxter and Jain, 1989; Baxter and Jain, 1990, 1991), and further developed by building in more complex and realistic processes to describe particular delivery strategies and systems (Tan et al., 2003; Tzafriri et al., 2005; Lee et al., 2005; Arifin et al., 2009; Nhan et al., 2014). A pharmacokinetics-based compartment model was used to evaluate the performances of free and liposomal *doxorubicin* under different delivery conditions (El-Kareh and Secomb, 2000). Systemic administration and implantable wafer were compared for *carmustine* based on a 3-D transport model in a realistic brain tumour (Wang et al., 1999).

In this study, a multiphysics model is applied to a 3-D brain tumour that is reconstructed from MR data, in order to examine the impacts of different factors on the liposome-mediated delivery of *temozolomide* for optimisation. The model describes the key transport processes, including plasma clearance, transvascular transport, convective and

diffusive transport in interstitial fluid, drug release from liposomes, binding with proteins, and drug elimination by metabolic reactions and degradation. Delivery outcomes are evaluated in terms of the drug bioavailability based on the predicted free *temozolomide* concentrations across time.

2. Material and methods

2.1. Mathematical model

The modelling framework consists of several submodules with equations for the drug delivery, including those for interstitial fluid flow in the brain and surrounding normal tissue, direct delivery of free *temozolomide* as control study and liposome-mediated delivery.

2.1.1. Interstitial fluid flow

Morphological characteristics of microvasculature network can vary considerably in brain tumour depending on the tumour type and stage. Given the inter-capillary distance is orders lower than the scale of drug transport in tissues (Baxter and Jain, 1989), the brain tumour and its holding tissue are treated as porous media where the microvasculature is assumed to be homogenously distributed (Baxter and Jain, 1990). The mass equation and momentum conservation equation for interstitial fluid flow are in the forms of

$$\nabla \cdot \mathbf{v} = F_b \tag{1}$$

$$\rho \left(\frac{\partial \mathbf{v}}{\partial t} + \mathbf{v} \cdot \nabla \mathbf{v} \right) = -\nabla p_i + \nabla \cdot \boldsymbol{\tau} - \left(\frac{\mu}{\kappa} \right) \mathbf{v} \tag{2}$$

in which $\mathbf{v}$ and p_i are the velocity and pressure of interstitial fluid flow, respectively. μ and ρ are the interstitial fluid viscosity and density, and κ refers to the tissue permeability. t is time, and $\boldsymbol{\tau}$ is the stress tensor. The fluid gain from blood circulatory system (F_b) is determined by the Starling's law as

$$F_b = K_b \frac{S}{V} [p_b - p_i - \sigma_T (\pi_b - \pi_i)] \tag{3}$$

where p_b stands for the blood pressure and K_b is the hydraulic conductivity of the microvasculature wall. S/V refers to the microvasculature surface area per tissue volume. σ_T is the osmotic reflection coefficient. π_b and π_i are the blood and interstitium osmotic pressure, respectively. The fluid loss to lymphatic system is ignored because of the lack of functional lymphatics in brain (Weller et al., 2009).

2.1.2. Direct delivery of free temozolomide

The transport processes of free *temozolomide* in tissue under directly delivery are illustrated in Fig. 1(a), and can be described by the equations of the drug concentration in blood and tissue, respectively. The intravascular concentration of free *temozolomide* strongly depends on the administration mode. For continuous infusion, the concentration (C_{IVS}) is governed by

$$\begin{cases} C_{IVS} = \frac{Dose}{T_d V_{F,d} k_{F,c}} (1 - e^{-k_{F,c}t}) & (t < T_d) \\ C_{IVS} = \frac{Dose}{T_d V_{F,d} k_{F,c}} (e^{k_{F,c} T_d} - 1) e^{-k_{F,c}t} & (t \geq T_d) \end{cases} \tag{4}$$

where *Dose* refers to the total dose of drugs administrated in the treatment. t is time and T_d is the infusion duration. $V_{F,d}$ and $k_{F,c}$ stand for the drug distribution volume and plasma clearance rate, respectively. The time course of drug intravascular concentration under oral administration can be expressed as

$$C_{IVS} = \frac{G k_{F,a} Dose}{V_{F,d} (k_{F,a} - k_{F,c})} (e^{-k_{F,c}t} - e^{-k_{F,a}t}) \tag{5}$$

in which G is the fraction of drugs that are absorbed through the digestive system, and $k_{F,a}$ is the absorption rate. Given free *temozolomide* can bind with proteins and the concentration of free and bound drugs

are able to reach equilibrium (Danson and Middleton, 2001), the intravascular concentration of free *temozolomide* ($C_{F,IVS}$) can be calibrated by

$$C_{IVS} = C_{F,IVS} + C_{B,IVS} = C_{F,IVS} (1 + K_{IVS}) \tag{6}$$

where $C_{B,IVS}$ is the intravascular concentration of bound *temozolomide*, and K_{IVS} is the binding constant.

Both the brain tumour and normal tissue could be divided as extracellular space (ECS), cell membrane (CM) and intracellular space (ICS). The concentration of free *temozolomide* in the entire tissue (C_F) is governed by the mass conservation equation (Arifin et al., 2009; Zhan and Wang, 2018) as

$$\frac{\partial C_F}{\partial t} = \alpha D_{F,ECS} \nabla^2 C_{F,ECS} - \nabla \cdot (\alpha \mathbf{v} C_{F,ECS}) + \alpha Ex(C_{F,IVS}, C_{F,ECS})$$
$$- \alpha k_{F,e} C_{F,ECS} - \beta k_{F,e} C_{F,ICS} - \frac{\partial C_B}{\partial t} \tag{7}$$

where $k_{F,e}$ is the free drug elimination rate. α and β denote the volume fraction of ECS and ICS, respectively. The exchange of free *temozolomide* between the intravascular space (IVS) and tissue ECS is defined as

$$Ex(C_{F,IVS}, C_{F,ECS}) = \left[F_b (1 - \sigma_F) C_{F,IVS} + P_F \frac{S}{V} (C_{F,IVS} - C_{F,ECS}) \frac{\text{Pe}_F}{e^{\text{Pe}_F} - 1} \right] \tag{8}$$

and the transvascular Péclet number is $\text{Pe}_F = \frac{F_b(1 - \sigma_F)}{P_F S / V}$.

Two assumptions are further introduced: (1) the equilibrium of free *temozolomide* concentration is reached among the three tissue compartments (Saltzman and Radomsky, 1991) ($P_{ICS-ECS} = C_{F,ICS}/C_{F,ECS}$; $P_{CM-ECS} = C_{F,CM}/C_{F,ECS}$) and (2) the concentration of free and bound drugs are linearly correlated (Eikenberry, 2009) ($K_{ECS} = C_{B,ECS}/C_{F,ECS}$; $K_{ICS} = C_{B,ICS}/C_{F,ICS}$). Therefore, Eq. (7) can then be simplified as

$$\frac{\partial C_{F,ECS}}{\partial t} = D_{F,ECS}^* \nabla^2 C_{F,ECS} - \mathbf{v}^* \cdot \nabla C_{F,ECS} - k_{F,e}^* C_{F,ECS}$$
$$+ Ex^*(C_{F,IVS}, C_{F,ECS}) \tag{9}$$

where $\mathbf{v}^* = (\alpha/\eta)\mathbf{v}$ is the apparent velocity of interstitial fluid flow. $D_{F,ECS}^* = (\alpha/\eta) D_{F,ECS}$ is the free drug apparent diffusivity. $k_{F,e}^* = [(\alpha + \beta) k_{F,e} + F_b]/\eta$ refers to the apparent drug elimination rate. $Ex^*(C_{F,IVS}, C_{F,ECS}) = \alpha Ex(C_{F,IVS}, C_{F,ECS})/\eta$ is the apparent exchange between IVS and ECS, and η is a drug dependent parameter which is given as

$$\eta = \alpha(1 + K_{ECS}) + \beta P_{ICS-ECS}(1 + K_{ICS}) + (1 - \alpha - \beta) P_{CM-ECS} \tag{10}$$

2.1.3. Delivery of liposome encapsulated temozolomide

The drug transport processes of liposome-mediated delivery are represented in Fig. 1(b). The intravascular concentration of liposomal drugs ($C_{L,IVS}$) under continuous infusion is governed by

$$\begin{cases} C_{L,IVS} = \frac{Dose}{T_d V_{L,d}(k_{L,c} + k_{rel,IVS})} [1 - e^{-(k_{L,c} + k_{rel,IVS})t}] & (t < T_d) \\ C_{L,IVS} = \frac{Dose}{T_d V_{L,d}(k_{L,c} + k_{rel,IVS})} [e^{(k_{L,c} + k_{rel,IVS})} - 1] e^{-(k_{L,c} + k_{rel,IVS})t} & (t \geq T_d) \end{cases} \tag{11}$$

where $V_{L,d}$ and $k_{L,c}$ are the distribution volume and plasma elimination rate of liposomes, respectively, and $k_{rel,IVS}$ is the drug release rate from liposomes in IVS. This concentration under bolus injection follows an exponential decay defined as

$$C_{L,IVS} = \frac{Dose}{V_{L,d}} e^{-(k_{L,c} + k_{rel,IVS})t} \tag{12}$$

The liposomal drug concentration in tissue ECS ($C_{L,ECS}$) is determined by the diffusive and convective transport with the interstitial fluid flow, drug release and exchange with IVS, as
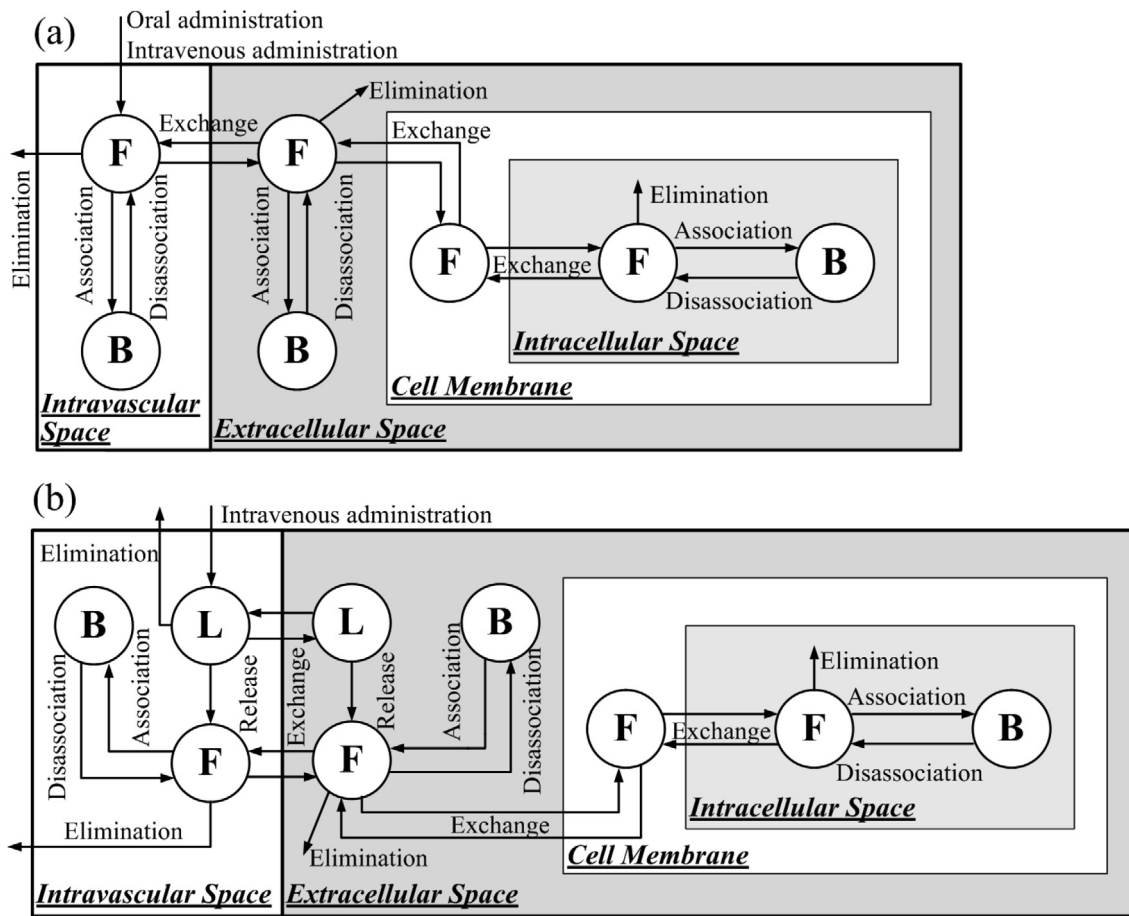
Fig. 1. Schematic diagrams for drug transport under different delivery modes. (a) Oral and intravenous administration of non-encapsulated *temozolomide*. (b) Intravenous administration of liposome encapsulated *temozolomide*. Letters of L, F and B refer to the liposome-encapsulated drugs, free drugs and the drugs that bind with proteins, respectively.
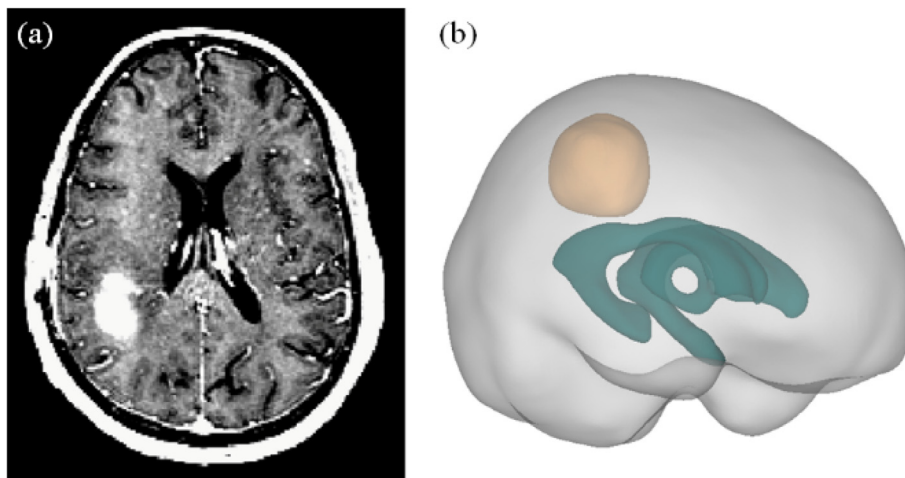

Fig. 2. Model geometry. (a) A representative slice of MR images. (b) The reconstructed 3D geometry, with tumour, ventricle and normal brain tissue highlighted in orange, dark green and grey, respectively. (For interpretation of the references to colour in this figure legend, the reader is referred to the web version of this article.)

$$\frac{\partial C_{L,ECS}}{\partial t} = D_{L,ECS}\nabla^2 C_{L,ECS} - \nabla\cdot(\mathbf{v}C_{L,ECS}) - k_{rel,ECS}C_{L,ECS}$$
$$+ Ex(C_{L,IVS}, C_{L,ECS}) \qquad (13)$$

where $D_{L,ECS}$ is the liposome diffusivity in tissue interstitial fluid flow, and $k_{rel,ECS}$ is the drug release rate from liposomes in tissue ECS.

Free *temozolomide* concentration in blood ($C_{F,IVS}$) is governed by the exchange with tissue, plasma clearance and drug release, as

$$\frac{\partial C_{F,IVS}}{\partial t} = k_{rel,IVS}C_{L,IVS} - \frac{V_{tissue}}{V_{F,d}}Ex(C_{F,IVS}, C_{F,ECS}) - k_{F,c}C_{F,IVS} - \frac{\partial C_{B,IVS}}{\partial t}$$
$$(14)$$

in which V_{tissue} stands for the volume of brain tumour or normal tissue, depending on the location. The free *temozolomide* concentration in tissue ECS ($C_{F,ECS}$) can be described in the form of

$$\frac{\partial C_{F,ECS}}{\partial t} = D_{F,ECS}^* \nabla^2 C_{F,ECS} - \mathbf{v}^* \cdot \nabla C_{F,ECS} - k_{F,e}^* C_{F,ECS}$$

$$+ Ex^*(C_{F,IVS}, C_{F,ECS}) + k_{rel,ECS}^* C_{L,ECS} \qquad (15)$$

where $k_{rel,ECS}^* = k_{rel,ECS}/\eta$ is the apparent drug release rate from liposomes.

2.2. Model geometry

The tumour and its surrounding normal brain tissue are reconstructed in 3-D from anonymous MR images, which are available on the image database of TCIA under the Creative Commons Attribution 3.0 Unported License for scientific purposes (Barboriak, 2015; Clark et al., 2013). The images were acquired in three orthogonal planes with slice thickness of 1 mm. Each slice comprises 256×256 pixels, and the pixel size is 1 mm. A representative slice is shown in Fig. 2(a).

The brain tumour is segmented from ventricle and normal brain tissue on each image slice with respect to the local signal intensity using MIMICS (Materialise HQ, Leuven, Belgium). Smoothed surfaces of the tumour, normal tissue and ventricle are imported into ANSYS ICEM CFD (ANSYS Inc., Canonsburg, USA) to generate the computation mesh, which consists of 4.6 million tetrahedral elements to provide the grid independent solutions. The tumour and normal brain tissue shown in Fig. 2(b) are 24.7 cm^3 and 1387.3 cm^3, respectively.

2.3. Model parameters

Geometric and transport properties are treated as time-independent because the simulation time window is much shorter than that of tumour growth. Tables 1 and 2 summarise the model parameters representing the properties of tissue and *temozolomide* in its different forms, respectively. The first order kinetics (Afadzi et al., 2010) is applied to analyse the accumulative releasing profile (Gao et al., 2015) for estimating the drug release rate in tissue ECS, while the liposomes are assumed to be stable in blood owing to the lack of experimental data (Gao et al., 2015). The averaged value of liposome transvascular permeability is found to be 2.20E-8 m/s in normal tissues by analysing the biodistribution profiles (Gao et al., 2015) based on the two-compartment model (Zhao et al., 2007). It is set as 5.84E-8 m/s in tumour as this parameter is usually 1.4–3.9 times higher than in normal tissue (Wu et al., 1993; Chauhan et al., 2012). Liposomes are further assumed to be impermeable to the BBB in normal brain tissue and cannot be taken up by cells directly.

2.4. Numerical methods

The mathematical model is implemented in a CFD code package ANSYS FLUENT (ANSYS Inc., Canonsburg, USA) for obtaining numerical solutions. Pressure is correlated with velocity correction by SIMPLEC algorithm. The 2nd order UPWIND scheme and the 2nd order implicit Euler scheme are applied to obtain the spatial and temporal

discretisation of governing equations, respectively. The residual tolerance of 1E-5 is chosen to control the modelling convergence, and a fixed time step is set as 10 s after time-step independent tests. As the impacts of intravenous administration on the interstitial fluid is ignorable (Goh et al., 2001), governing equations of interstitial fluid flow are solved first to generate a steady-state solution. The obtained fluid pressure and velocity are imported to the drug transport model at time zero for transient simulations of drug delivery (Zhao et al., 2007; Gasselhuber et al., 2012; Soltani and Chen, 2013). Drug concentrations are assumed to be zero in the whole domain as the initial condition.

2.5. Boundary conditions

Relative pressure of 1447 Pa (Kimelberg, 2004) and 658 Pa (Gross and Popel, 1979) are specified on the brain and ventricle surface, respectively, where there is no drug flux. All the variables are continuous across the interface between the brain tumour and its holding tissue.

3. Results

3.1. Hydraulic environment for drug delivery

Drug transport and accumulation strongly depend on the hydraulic environment in tissues, including the interstitial fluid pressure (IFP) and velocity (IFV). The interstitial fluid flow is predicted by solving the governing equations in the entire domain, subjected to model parameters in Table 1 and the aforementioned boundary conditions. Results in Fig. 3 shows that IFP decreases from the ventricle towards the brain surface in normal tissue, driving the interstitial fluid to flow in the same direction (Abbott, 2004). However, the increased microvasculature density and hydraulic conductivity of the vessel wall are able to improve the fluid leakage from IVS to ECS in the brain tumour, and thereby build up the IFP and IFV locally (Jain, 1987). This advanced fluid loss could increase the drug gain from blood stream to enhance the drug accumulation. Moreover, the convective drug transport can also be improved because of the high IFV in the brain tumour.

It is worth to note that the interstitial fluid flow is heterogeneous in the brain tumour. IFP is slightly higher in the deep tumour tissue near the ventricle. This raised IFP is able to reduce the pressure gradient across the vessel wall and thereby inhibits the fluid loss from blood locally. The bulk movement of interstitial fluid flow is found to be faster in the tumour region that is close to the normal tissue surface, owing to the large pressure difference there as shown in Fig. 3.

3.2. Baseline study of drug transport and accumulation

A total dose of 150 mg/m^2 liposome encapsulated *temozolomide* (Kushner et al., 2006) is administrated into a 70 kg patient (Goh et al., 2001) through 1.5-h intravenous infusion (Diez et al., 2010). Delivery outcomes are compared to control studies in which the identical dose of non-encapsulated *temozolomide* is delivered by oral administration and

Table 1
Parameters for the brain tumour and normal tissue.

Symbol	Parameter	Unit	Brain Tumour	Normal Tissue
α	Volume fraction of extracellular space	–	0.35 (Kalyanasundaram et al., 1997)	0.20 (Fung et al., 1996)
β	Volume fraction of intracellular space	–	0.55 (Kalyanasundaram et al., 1997)	0.65 (Fung et al., 1996)
ρ	Interstitial fluid density	kg/m^3	1000 (Green and Perry, 1973)	1000 (Green and Perry, 1973)
μ	Interstitial fluid viscosity	kg/m/s	7.8E-4 (Green and Perry, 1973)	7.8E-4 (Green and Perry, 1973)
π_b	Blood osmotic pressure	Pa	3440 (Kimelberg, 2004)	3440 (Kimelberg, 2004)
π_i	Interstitium osmotic pressure	Pa	1110 (Baxter and Jain, 1989)	740 (Baxter and Jain, 1989)
p_b	Pressure in intravascular space	Pa	4610 (Kimelberg, 2004)	4610 (Kimelberg, 2004)
S/V	Area of vessel surface per tissue volume	m^{-1}	20,000 (Baxter and Jain, 1989)	7000 (Baxter and Jain, 1989)
σ_T	Osmotic reflection coefficient	–	0.82 (Baxter and Jain, 1989)	0.91 (Baxter and Jain, 1989)
K_b	Hydraulic conductivity of the blood vessel wall	m/Pa/s	1.1E-12 (Arifin et al., 2009)	1.4E-13 (Arifin et al., 2009)
κ	Darcy's permeability	m^2	6.4E-14 (Arifin et al., 2009)	6.5E-15 (Arifin et al., 2009)

Table 2
Parameters for chemotherapeutic drugs[*].

Symbol	Parameter	Unit	Liposome	Temozolomide
$P_{ICS\text{-}ECS}$	Partition coefficient between ICS and ECS	–	–	1.0 (Fung et al., 1996)
$P_{CM\text{-}ECS}$	Partition coefficient between CM and ECS	–	–	1.5E-2 (Yang et al., 2018)
$K_{IVS}, K_{ECS}, K_{ICE}$	Protein binding constant in IVS, tissue ECS and ICS	–	–	1.8E-1 (Danson and Middleton, 2001)
D_{ECS}	Diffusivity in extracellular space	m^2/s	1.53E-13 (T) (Zhang et al., 2008) 3.21E-14 (N) (Ziemys et al., 2016)	7.2E-10[#] (T) (Zhan et al., 2014) 3.4E-10[#] (N) (Swabb et al., 1974)
P	Transvascular permeability	m/s	5.84E-8 (T) (Gao et al., 2015) (E-7–E-11)[†] (Chauhan et al., 2012; Schmidt and Wittrup, 2009) 0.0 (N)	8.0E-8 (T) (Rosso et al., 2009) 4.3E-8 (N) (Rosso et al., 2009)
σ	Osmotic reflection coefficient	–	0.95 (T) (Zhan and Xu, 2013) 1.0 (N) (Zhan and Xu, 2013)	0.15 (T) (Goh et al., 2001) 0.15 (N) (Goh et al., 2001)
G	Fraction absorbed in oral administration	–	–	1.0 (Baker et al., 1999)
k_e	Drug elimination rate	s^{-1}	–	1.06E-4 (Friedman et al., 2000)
k_c	Plasma clearance rate	s^{-1}	8.13E-5 (Gao et al., 2015)	1.06E-4 (Rosso et al., 2009)
k_a	Absorption rate in oral administration	s^{-1}	–	5.75E-04 (Diez et al., 2010)
$k_{rel,IVS}$	Release rate in IVS	s^{-1}	0.0 (Gao et al., 2015) (0~E-6)[†] (Tagami et al., 2011; Connor et al., 1984; Garcion et al., 2006; Tagami et al., 2012)	–
$k_{rel,ECS}$	Release rate in tumour ECS	s^{-1}	6.42E-4 (Gao et al., 2015) (E-2–E-6)[†] (Tagami et al., 2011; Connor et al., 1984; Garcion et al., 2006; Tagami et al., 2012)	–
V_d	Distribution volume	m^{-3}	2.20E-2 (Gao et al., 2015)	2.66E-2 (Diez et al., 2010)

[*] T and N refer to the tumour and normal tissue, respectively.
[†] Range of the parameter scale.
[#] Estimated based on the drug molecular weight.

intravenous administration with the same infusion duration.

Liposome encapsulated *temozolomide* concentration is crucial to determine the free drug accumulation in the brain tumour for effective therapy. Shown in Fig. 4 are the predicated time courses of liposomal *temozolomide* concentration in IVS and ECS of the brain tumour and its holding tissue. As all the liposomes are continuously administrated into blood, the concentration reaches the peak at 1.5 h and keeps decreasing with time proceeding. Its concentration in tumour ECS increases rapidly in the initial phase because of the large concentration gradient across the blood vessel wall, and then reaches the peak when the equilibrium is established between the source term of drug supply from blood stream and the sink term accounting for the continuous release. The gradual fall of concentration in tumour ECS is contributed by the decrease of IVS concentration and the drug release from liposomes. Since the liposomes are too large to cross the BBB, liposomal *temozolomide* enters the normal tissue mainly by convection and diffusion from the brain tumour. So that its concentration is about 2 orders lower than in the tumour.

The spatial distribution of liposomal and free *temozolomide* at different time points are compared in Fig. 5. Regardless the drug form, *temozolomide* is uniformly distributed except at the tumour/normal-tissue interface where a large concentration gradient presents. The peak liposomal drug concentration takes place at 1.5-h when the infusion ends, whereas, free drug concentration reaches a higher level at around 3.0-h. This is because although the liposome concentration decreases once after the infusion caseation, the free drug supply of releasing is still greater than the drug elimination, leading the free drug concentration to keep increasing. Since the free drug supply decreases with the liposome concentration as time proceeds, the drug elimination becomes dominant at around 3 h and the free drug concentration begins to decline.

Predicted free *temozolomide* concentrations for liposome-mediated delivery and non-encapsulated *temozolomide* delivery are compared in Fig. 6. Results show that the IVS concentration by oral administration is
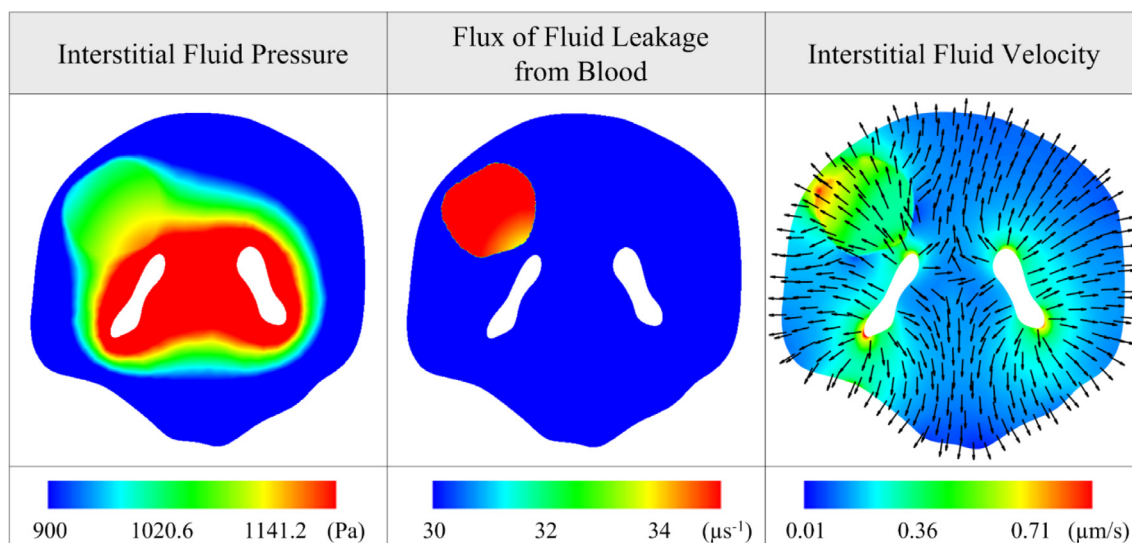

Fig. 3. Hydraulic environment in the brain tumour and its surrounding normal tissue.
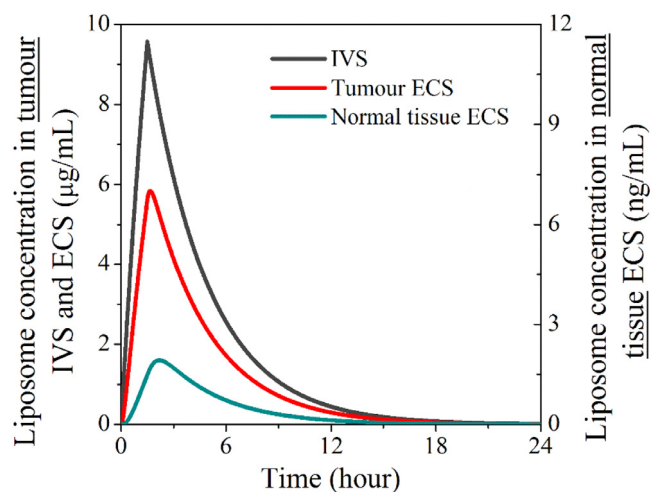
Fig. 4. Liposomal *temozolomide* concentration in IVS and ECS of the tumour and its surrounding normal tissue as a function of time.

close to that of intravenous administration in which non-encapsulated *temozolomide* are directly infused into blood. This can be attributed to the high systemic availability of *temozolomide* that enables nearly 100% drugs (Baker et al., 1999) being absorbed by the digestive system to enter the IVS. As a result of being well encapsulated, the free drug IVS concentration in liposome-mediated delivery maintains at a fairly low level over time. This is different from the delivery results in the tumour ECS, where comparable free *temozolomide* concentrations are found for all the examined delivery modes. Further comparisons denote that liposome-mediated delivery can rise the concentration peak and maintain the concentration at a relatively higher level in the decreasing phase, and thereby improves the drug accumulation for effective therapy.

Results in Fig. 6(c) show that the free *temozolomide* concentration can be largely reduced in normal tissue ECS in liposome-mediated delivery. The free drug supplies by transvascular transport and local release are low, due to the small amount of liposomes concentrating in IVS and normal tissue ECS as shown in Figs. 4 and 6(a). Such that free drugs entering the normal tissue mainly relies on the migration from tumour ECS. On the contrary, the large concentration gradient across vessel wall leads to the significant drug accumulation in normal tissue ECS in non-encapsulated drug delivery.

The bioavailability of anticancer drugs for producing biological

effects can be measured by the drug exposure across time, which is defined as area under the curve of free *temozolomide* concentration (*AUC*). The delivery outcomes of each mode are compared in terms of 24-h *AUC* in different compartments in Table 3. Results show that liposome-mediated delivery can successively improve the drug bioavailability in tumour ECS whilst reducing the exposure of blood stream and normal tissue to free drugs in orders. This is beneficial to improve the treatment efficacy against tumour and lower the risk of adverse effects simultaneously, and hence achieve the targeted therapy.

3.3. Effect of liposome transvascular permeability (P_L)

Transvascular permeability refers to the capacity of liposomes to cross the microvasculature wall. It has been found to vary in a wide range of E-7 ~ E-11 m/s in both the *in vivo* experiments (Chauhan et al., 2012) and theoretical analyses (Schmidt and Wittrup, 2009), presenting strong dependences on the liposome dimension, location and type of tumours, pore size on vessel wall and duration after infusion, *etc*. Therefore, the influence of P_L is examined in the range of 5.84E-7–5.84E-11 m/s in this study.

The effects of liposome transvascular permeability on *temozolomide* concentration are shown in Fig. 7. As the liposome distribution volume is orders higher than the tumour size (2.20E-2 m^3 *vs.* 2.47E-5 m^3), the impact of P_L on the liposome IVS concentration is ignorable. It is not surprising that the liposome concentration in tumour ECS can be largely improved by increasing P_L since more drugs can transport into the tumour tissue. As a result, free drug concentration in tumour is risen so as to improve the treatment efficacy. Similar effects can be found on free drug concentrations in IVS and normal tissue ECS, because the accumulation of free *temozolomide* in these two compartments are determined by the drug convective and diffusive transport from tumour ECS.

Delivery outcomes (*AUC*) under different liposome transvascular permeability values are compared in Fig. 7. Results show that the free drug bioavailability is non-linearly related to liposome transvascular permeability, indicating the increase of P_L could present a saturable effect on the overall drug exposure in all the studied compartments. It is worth to note that the delivery outcomes in blood and normal tissue share the similar patterns as in the tumour, suggesting that increasing liposome permeability could not only improve the treatment efficacy but also result in higher risks of adverse effects.
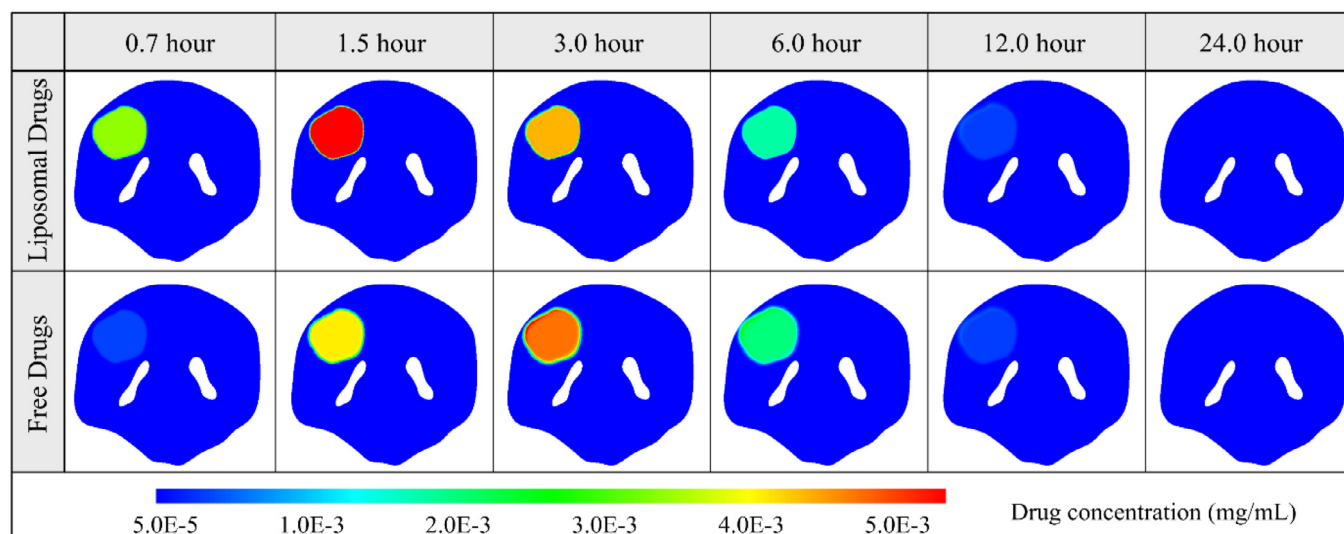

Fig. 5. Spatial distribution of *temozolomide* concentration at different time points under 1.5-h continuous infusion.
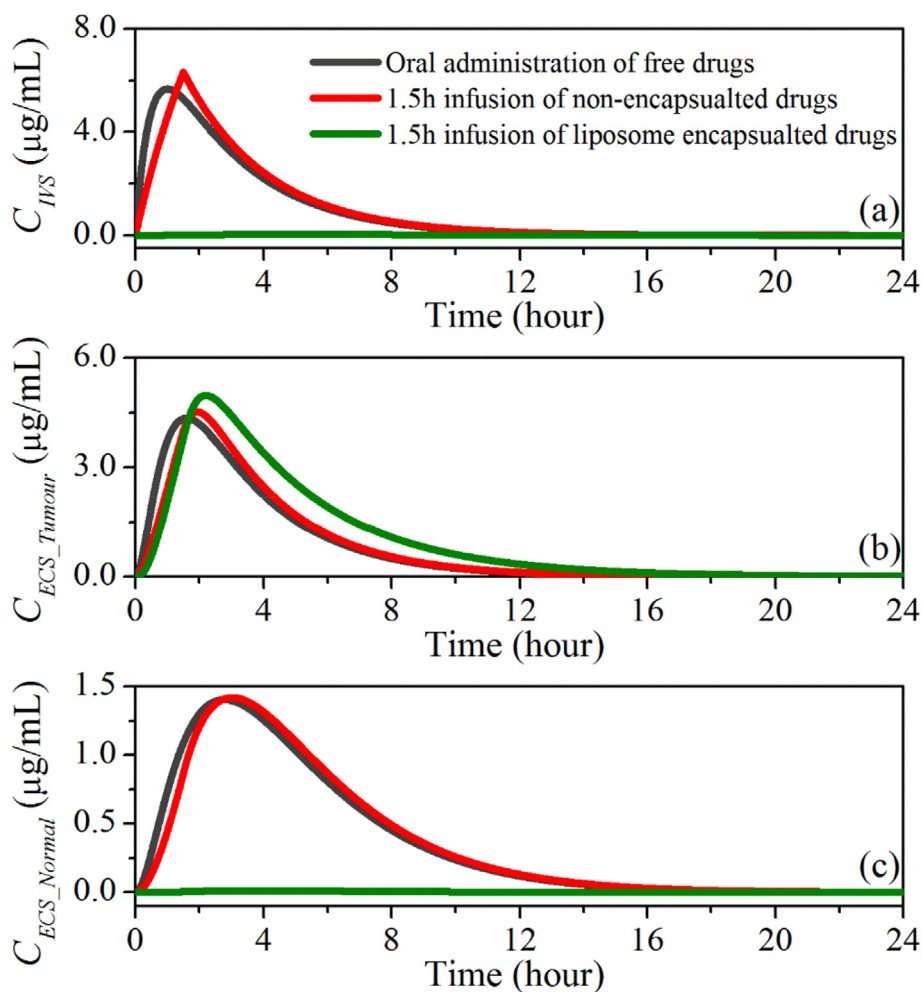
Fig. 6. Free *temozolomide* concentration as a function of time under different delivery modes in (a) IVS, (b) tumour ECS and (c) normal tissue ECS.

Table 3
AUC_{24h} of different delivery modalities (mg/mL·h).

	Oral Administration of non-encapsulated drugs	1.5 h infusion of non-encapsulated drugs	1.5 h infusion of liposomal drugs
Blood stream (IVS)	2.177E-2	2.177E-2	3.428E-4
Tumour ECS	1.842E-2	1.844E-2	2.497E-2
Normal tissue ECS	8.750E-3	8.748E-3	9.367E-5

3.4. Effect of extravascular release rate ($k_{rel,ECS}$)

Release rate is a key parameter determining the toxicity and activity of liposomal delivery system. It stands for the time scale for liposomes to release the effective load of drugs, and depends on multiple factors including the liposome formulation, fabrication approach, temperature and environmental pH value (Tagami et al., 2011; Connor et al., 1984); *etc*. Stealth liposomes are able to provide sustainable drug release which may last for weeks (Garcion et al., 2006), whilst the loads of thermo-sensitive liposomes can be fully released in few seconds (Tagami et al., 2012). Therefore, the drug release rate in tissue ECS is varied in the range from 6.42E-6 to 6.42E-2 s^{-1} to study its effects.

As shown in Fig. 8, using fast release liposomes can significantly accelerate the free drug accumulation in tumour ECS to reach higher peaks, and further slowdown the concentration decrease after the in-fusion ends. This is able to provide sustainable drug supply to enhance the tumour cell killing. However, the free drug concentration in blood can be consequentially elevated, as the enlarged concentration gradient may drive more drugs to transport into the blood circulatory system.

Similar patterns can be found in normal tissue since the load of free drugs can also be efficiently released to form high concentrations.

Delivery outcomes are accounted by *AUC* in different tissue com-partments for each treatment using liposomes with different extra-cellular release rates. Quantitative comparisons show that increasing the drug extracellular release rate up to the scale of E-3 s^{-1} can largely improve the exposure of brain tumour to free *temozolomide*, while fur-ther increasing leads to less contributions. Similar findings on the blood stream and normal tissue indicate that the fast extracellular release is possible to introduce more serious adverse effects.

3.5. Effect of intravascular release rate ($k_{rel,IVS}$)

For well-designed liposomes that are stable in blood, encapsulated drugs cannot be released until entering the tumours. However, this is difficult to be achieved *in vivo* due to the metabolic processes and physical degradation, *etc*. In order to examine the effects of drug release in blood, delivery outcomes of liposomes with different intravascular release rates (5.84E-6 ~ 5.84E-3 s^{-1}) are compared to the control study
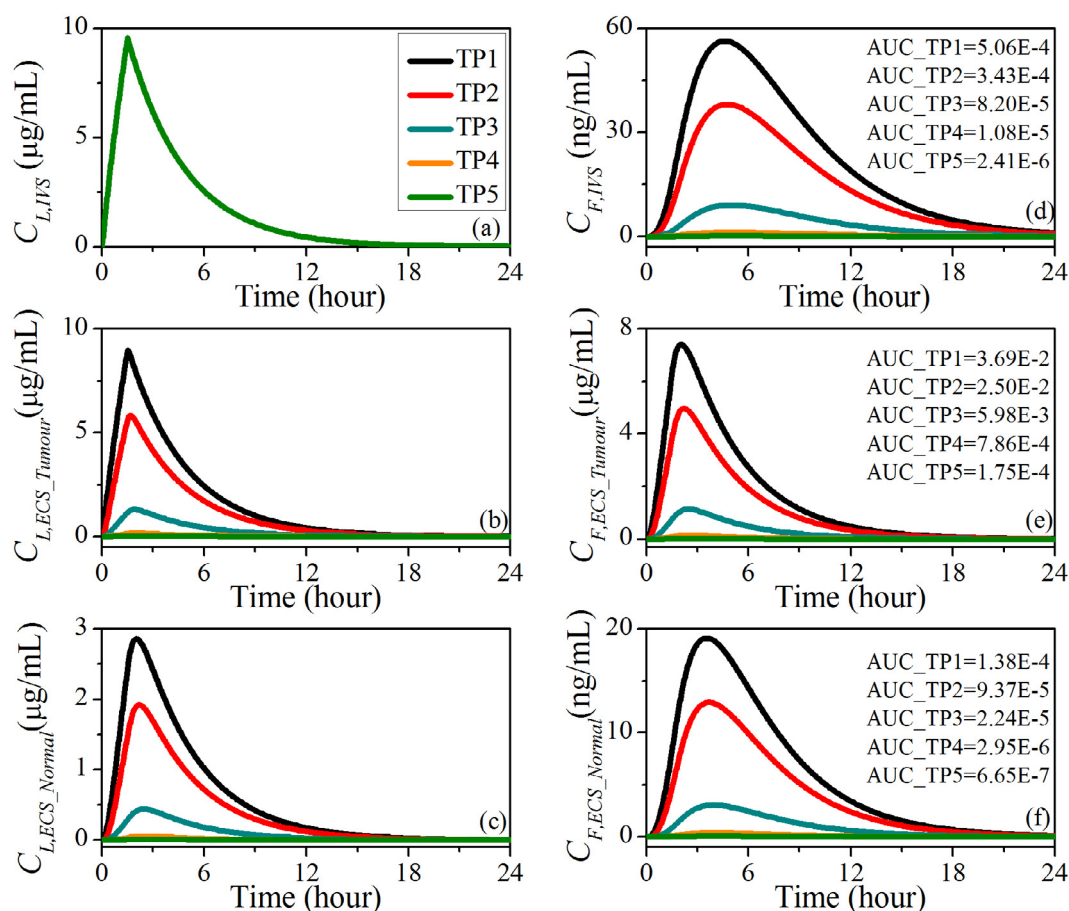
Fig. 7. Time courses of *temozolomide* concentrations using liposomes with different transvascular permeability values (P_L). Liposomal drugs in (a) IVS, (b) tumour ECS and (c) normal tissue ECS; free drugs in (d) IVS, (e) tumour ECS and (f) normal tissue ECS. TP1: P_L = 5.84E-7 m/s. TP2: P_L = 5.84E-8 m/s, TP3: P_L = 5.84E-9 m/s, TP4: P_L = 5.84E-10 m/s, TP5: P_L = 5.84E-11 m/s. AUC of each delivery in the corresponding compartment is given beside, with the unit of mg/mL·h.

in which the well-designed liposomes are used.

The impacts of intravascular release on *temozolomide* concentrations are shown in Fig. 9. Results denote that intravenous release can significantly reduce the liposome concentration in all the compartments, and effectively improve the free drug accumulation in blood to enlarge the concentration difference across the vessel wall. However, the impact on free drug concentration in tumour ECS is found to be relatively small. This is because on the one hand, the enlarged transvascular concentration gradient enables more free drugs transporting from blood into tumour ECS; on the other hand, there are less free drugs being released from liposomes owing to the reduced local liposome concentration. To be different, the free drug concentration in normal tissue increases with the intravascular release rate, because the liposome concentration there is low and the net gain of free drugs from blood is in domination.

The treatments using liposomes with different intravascular release rates are given in Fig. 9 in terms of *AUC*. Similar drug bioavailability in tumour ECS indicate that intravascular release has less impacts on the treatment efficacy against brain tumour. However, the risk of adverse effects could be significantly risen by the fast intravascular release owing to the high drug concentration in blood and normal tissue.

3.6. Effect of infusion duration (T_d)

Infusion duration is a factor that can be well controlled in clinical treatments. The delivery by bolus injection and continuous infusions lasting for 0.5, 1.5, 3.0 and 4.5 h are compared in this study. Fig. 10 shows that drug concentrations in different compartments share the

similar trends: prolonging the infusion duration could result in slow drug accumulation at the beginning of treatments to reach lower peaks, whilst the concentrations fall more gradually after the infusion ends. Quantitative analyses demonstrate that infusion duration has no obvious influence on the free *temozolomide* exposure in blood circulatory system, the brain tumour and its surrounding normal tissue.

4. Discussion

A multiphysics model is developed in this study to predict the temporal and spatial profiles of liposome-mediated delivery of *temozolomide* into brain tumour. Modelling predictions reveal the advantages of liposomes in effectively reducing the risk of adverse effects caused by the high free drug concentration in blood and normal tissue, and enhancing the drug accumulation in tumour site to improve the treatment efficacy. Comparisons also denote that oral administration of non-encapsulated *temozolomide* can result in similar drug accumulation as intravenous infusion, owing to the high systemic availability rate of free *temozolomide* (Newlands et al., 1997; Ostermann et al., 2004). This finding consists with the measurements in clinic (Newlands et al., 1992).

Modelling predictions indicate that increasing the liposome transvascular permeability (P_L) and extracellular release rate ($k_{rel,ECS}$) are effective routes to improve the treatment, however, the probabilities of adverse effects can be simultaneously risen. Further quantitative analyses show that although the drug bioavailability in blood and normal tissue increase with P_L and $k_{rel,ECS}$, their values are still orders lower than those in non-encapsulated drug delivery. This is different from
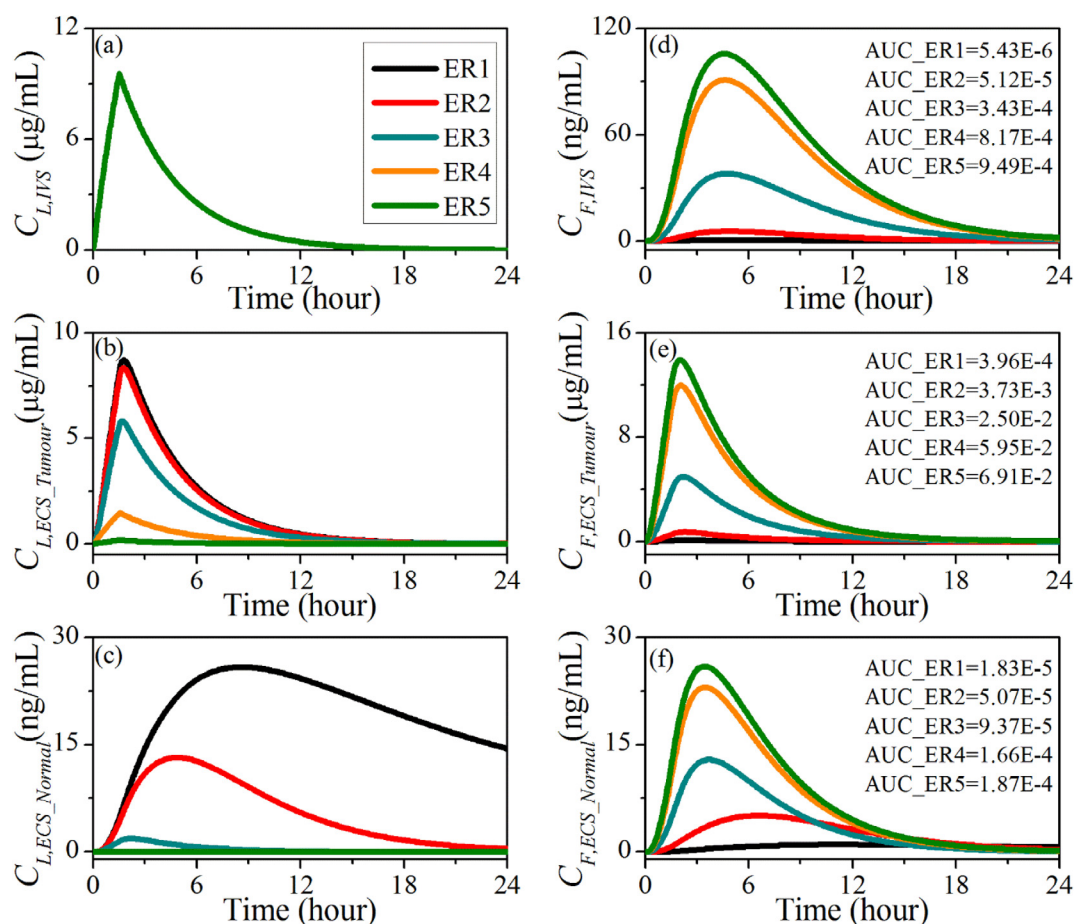
Fig. 8. Time courses of *temozolomide* concentrations using liposomes with different extracellular release rates ($k_{rel,ECS}$). Liposomal drugs in (a) IVS, (b) tumour ECS and (c) normal tissue ECS; free drugs in (d) IVS, (e) tumour ECS and (f) normal tissue ECS. ER1: $k_{rel,ECS} = 6.42E\text{-}6\,s^{-1}$, ER2: $k_{rel,ECS} = 6.42E\text{-}5\,s^{-1}$, ER3: $k_{rel,ECS} = 6.42E\text{-}4\,s^{-1}$, ER4: $k_{rel,ECS} = 6.42E\text{-}3\,s^{-1}$, ER5: $k_{rel,ECS} = 6.42E\text{-}2\,s^{-1}$. AUC of each delivery in the corresponding compartment is given beside, with the unit of mg/mL·h.

intravenous release, which could lead to comparable *AUC* in blood and normal tissue as in the delivery where free *temozolomide* is directly administrated into the blood stream.

Spatiotemporal profiles of free *temozolomide* are found to be highly dependent on the transport and accumulation of liposomes, indicating the treatment could be improved by optimising the liposome properties. Using liposomes with small dimension could be feasible to improve the delivery outcomes as the small size can significantly increase the transvascular permeability to enable more drugs entering the tumour ECS (Chauhan et al., 2012). This improvement could also be achieved by modifying the liposome surface with ligands (Kulkarni and Feng, 2011; Johnsen and Moos, 2016; Singh et al., 2016) or rising the local temperature (Dalmark and Storm, 1981). pH-sensitive liposomes (Kanamala et al., 2016) and thermosensitive liposomes coupled with local hyperthermia (Gasselhuber et al., 2012) can be applied to enhance the drug release within the tumour for improved cell killing while reducing the side effects in normal tissue. Moreover, liposomes should be carefully designed to improve their stability in blood stream, as the intravenous release can only increase the risk of adverse effects rather than the drug bioavailability in tumour. This is different from doxorubicin whose permeability is orders higher than that of liposomes in general tumours. As such intravascular release could result in more doxorubicin passing through the vessel wall for better accumulation in the tumour ECS (Gasselhuber et al., 2012).

Liposomes are capable of directly penetrating into tumour cells by means of endocytosis (Maurer et al., 2001) and thereby release the drugs locally for highly targeted treatment. However in intravenous

administration, liposomes are commonly modified by *polyethylene glycol* (PEG) in order to reduce the plasma clearance for obtaining sustainable drug supply. This ligand attached on liposome surface can successfully build up a steric barrier that is efficient in retarding the liposome interactions with cells and hence inhibit endocytosis (Miller et al., 1998; Vertut-Doï et al., 1996). Additionally, experiments have reported that liposomes with size greater than 80 nm are difficult to be endocytosed by tumour cells (Hatakeyama et al., 2004). Since this study mainly focuses on the delivery mode of intravenous administration, liposomes are assumed to be impenetrable to cells and endocytosis is neglected. This active transport process of liposome uptake by cells can be included by developing the mathematical model with experimental supports in the future.

The performances of mathematical model in predicting drug delivery to solid tumours have been compared to experimental results for validation. The model predicted IFV of 0.17 μm/s (Baxter and Jain, 1989) was well located in the experimental range of 0.13–0.2 μm/s (Butler et al., 1975). IFP was modelled as 1500 Pa and 40 Pa in the solid tumour and normal tissue (Zhan et al., 2014), respectively, which were within the corresponding ranges of 586.67–4200 Pa (Boucher and Jain, 1992) and −400 to 800 Pa (Raghunathan et al., 2010) obtained from experimental measurements. The drug transport model was applied to simulate the distribution volume of albumin and Evans blue in gel, with coefficients of multiple determination (R^2) of 0.83 and 0.7 achieved, respectively, as compared to the experiments (Neeves et al., 2006). Comparisons to animal experiments indicate the modelling results of free drug delivery still remain qualitative (Bhandari et al., 2017;
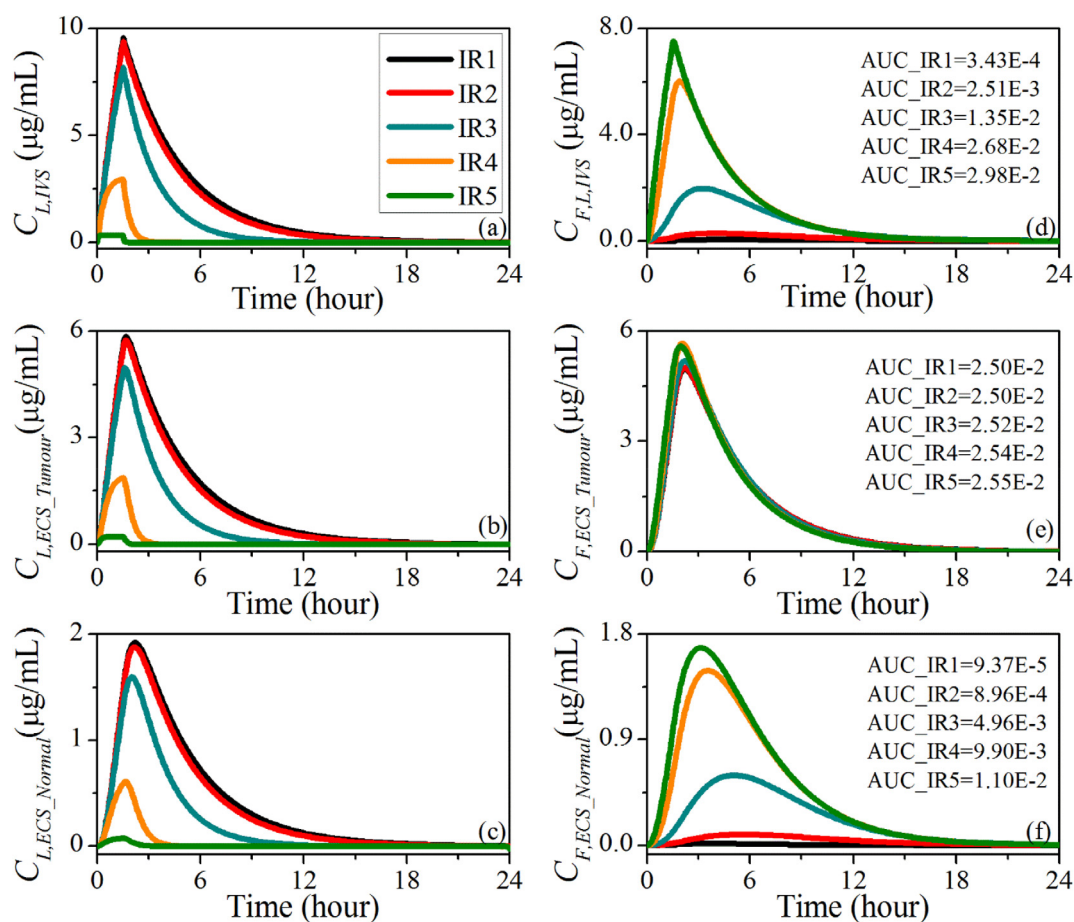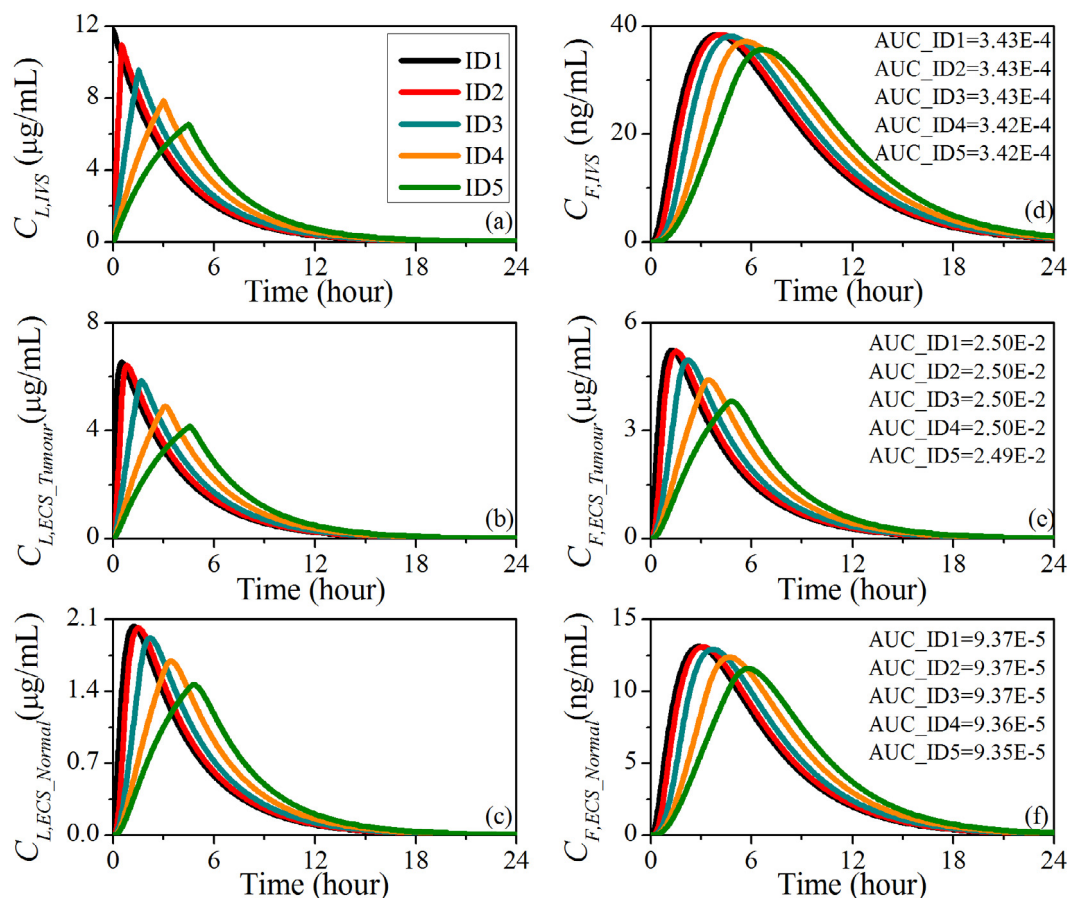
Fig. 9. Time courses of *temozolomide* concentrations using liposomes with different intravascular release rates ($k_{rel,IVS}$). Liposomal drugs in (a) IVS, (b) tumour ECS and (c) normal tissue ECS; free drugs in (d) IVS, (e) tumour ECS and (f) normal tissue ECS. IR1: $k_{rel,IVS} = 0.0\,\text{s}^{-1}$, IR2: $k_{rel,IVS} = 6.42\text{E-6}\,\text{s}^{-1}$, IR3: $k_{rel,IVS} = 6.42\text{E-5}\,\text{s}^{-1}$, IR4: $k_{rel,IVS} = 6.42\text{E-4}\,\text{s}^{-1}$, IR5: $k_{rel,IVS} = 6.42\text{E-3}\,\text{s}^{-1}$. AUC of each delivery in the corresponding compartment is given beside, with the unit of mg/mL·h.

Ranganath et al., 2010), whereas, the model predictive power can be largely improved for simulating the transport of nanoparticles as indicated by the quantitative comparison with *in vivo* data (Zhan and Wang, 2018). The heterogeneous, anisotropic properties of tumours and complex, controversial biophysical processes feature as the main obstacles for modelling the drug delivery. The predication accuracy can be improved by updating the input parameters with values measured in *in vivo* experiments, and biophysical and biochemical studies could provide insight to understand the drug delivery processes for model development.

The employed mathematical model involves several assumptions and limitations. (1) The lipid layer of liposomes in generic formulated products could fuse with cell membranes, thereby enabling liposomes to cross the vasculature wall (Kulkarni and Shaw, 2015). This membrane fusion has been found to depend on several factors, including the liposome size, distance between the lipid layers of liposomes and vessel wall, lipid composition and proteins (*i.e.* SNARE) (Chernomordik and Kozlov, 2008). In order to simulate the delivery with reduced side effects caused by the drug accumulation in normal tissue, the examined liposomes are assumed to be penetrable to the tumour microvasculature only, whilst the transvascular transport in normal tissue is neglected. As a result, results obtained in this study are valid only for the liposomes that do not fuse with cell membranes. (2) In order to focus on the drug transport in the entire tumour and brain tissue, microvasculature is modelled as the source term in governing equations given the vessel diameter is orders smaller than the tumour dimension. So that the effect of vessel geometric features on delivery outcomes are not included. This impact could be examined using microscale transport models where

vasculature network is modelled explicitly (Soltani and Chen, 2013). (3) Liposome diffusion coefficients in tumour and its surrounding normal tissue can vary simultaneously with respect to the liposome shape, size and formulation, (Zhang et al., 2008; Ziemys et al., 2016; Dewhirst and Secomb, 2017) *etc.* However, given there is lack of mathematical model describing this synchronous variation, the effect of liposome diffusivity is not addressed. Experimental data is needed to setup the corresponding model for the subsequent studies. (4) Microvasculature is assumed to be homogenously distributed in the brain tumour and its surrounding normal tissue (Baxter and Jain, 1989; Goh et al., 2001; Soltani and Chen, 2013); owing to the lack of relative information that can be extracted from the adopted MR images. As a consequence, model predictions from this study correspond to the generic, averaged delivery outcomes in the entire tumour and its holding tissue, not location-specified. This assumption can be relaxed by combing the model with advanced medical imaging techniques, such as dynamic contrast-enhanced imaging (Zhao et al., 2007) to obtain the local microvascular density. Microscopic imaging can also be applied to reconstruct the 3-D structure of capillary network for investigating the drug transport by means of microscale-transport modelling (Eikenberry, 2009). (5) The biological and geometric properties of the brain tumour and its holding tissue, as well as the transport properties of liposomes and free *temozolomide* are assumed to be independent of time. This is owing to the simulation time window is much shorter as compared to the time constant of tumour growth (Baxter and Jain, 1989). The changes of these properties with time should be included into the modelling studies for long term treatments, where the tumour can significantly develop. (6) The dynamic variation of interstitial fluid

Fig. 10. Time courses of *temozolomide* concentrations under different infusion durations (T_d). Liposomal drugs in (a) IVS, (b) tumour ECS and (c) normal tissue ECS; free drugs in (d) IVS, (e) tumour ECS and (f) normal tissue ECS. ID1: $T_d \approx 0.0$ h (bolus injection), ID2: $T_d = 0.5$ h, ID3: $T_d = 1.5$ h, ID4: $T_d = 3.0$ h, ID5: $T_d = 4.5$ h. AUC of each delivery in the corresponding compartment is given beside, with the unit of mg/mL·h.

flow is ignored through the entire drug delivery process. This is because on the one hand, the impact of intravenous administration is less than 3% and can be eliminated in a rather short time window as compared to the treatment duration (Goh et al., 2001); on the other hand, the drug solution is diluted so that the influence on the interstitial fluid properties, such as viscosity, can be ignored (Baxter and Jain, 1989). The time course of interstitial fluid flow should be incorporated for simulating the delivery of drugs that are able to largely change properties of the biological system.

The mathematical model is developed to describe the key biophysical and physicochemical processes in drug delivery to brain tumour. The adopted model parameters refer to the averaged and representative values obtained from literature. Therefore, modelling predictions are able to provide qualitative comparisons of the delivery outcomes under different conditions. Findings from this study enable identifying the contributions of each factor to the delivery so as to provide suggestions for optimising liposome properties and delivery strategy for improvement. Patient-specific and liposome-specific studies could be carried out with the supports from medical imaging and extensive experiments.

5. Conclusions

Delivery of liposome encapsulated *temozolomide* into brain tumour has been studied by means of mathematical modelling based on a 3-D realistic tumour reconstructed from medical images. As compared to the routine delivery using free *temozolomide*, liposome-medicated delivery is capable of improving the drug bioavailability in tumour while significantly reducing the risk of adverse effects. Delivery outcomes are less sensitive to the duration of intravenous administration but present

strong dependences on liposome properties. Modelling results demonstrate that the treatment can be benefited by increasing either the liposome transvascular permeability or the release rate in tumour extracellular space, whereas, releasing *temozolomide* in blood stream could only rise the risk of adverse effects. Findings from this study could be used as a guild for the design of liposome-mediated delivery of *temozolomide*.

Declaration of interests

The author declares that there is no known competing financial interests or personal relationships that could have appeared to influence the work reported in this paper.

References

Abbott, N.J., 2004. Evidence for bulk flow of brain interstitial fluid: significance for physiology and pathology. Neurochem. Int. 45, 545–552.

Afadzi, M., Davies, C.d.L., Hansen, Y.H., Johansen, T.F., Standal, Ø.K.-V., Måsøy, S.-E., Angelsen, B., 2010. Ultrasound stimulated release of liposomal calcein. Ultrasonics Symposium (IUS) IEEE 2107–2110.

Arifin, D.Y., Lee, K.Y.T., Wang, C.-H., 2009. Chemotherapeutic drug transport to brain tumor. J. Control. Release 137, 203–210.

Baker, S.D., Wirth, M., Statkevich, P., Reidenberg, P., Alton, K., Sartorius, S.E., Dugan, M., Cutler, D., Batra, V., Grochow, L.B., 1999. Absorption, metabolism, and excretion of 14C-temozolomide following oral administration to patients with advanced cancer. Clin. Cancer Res. 5, 309–317.

Barboriak, D., 2015. Data From RIDER_NEURO_MRI. The Cancer Imaging Archive.

Baxter, L.T., Jain, R.K., 1989. Transport of fluid and macromolecules in tumors. I. Role of interstitial pressure and convection. Microvasc. Res. 37, 77–104.

Baxter, L.T., Jain, R.K., 1990. Transport of fluid and macromolecules in tumors. II. Role of heterogeneous perfusion and lymphatics. Microvasc. Res. 40, 246–263.

Baxter, L.T., Jain, R.K., 1991. Transport of fluid and macromolecules in tumors: III. Role

of binding and metabolism. Microvasc. Res. 41, 5–23.

Bhandari, A., Bansal, A., Singh, A., Sinha, N., 2017. Perfusion kinetics in human brain tumor with DCE-MRI derived model and CFD analysis. J. Biomech. 59, 80–89.

Boucher, Y., Jain, R.K., 1992. Microvascular pressure is the principal driving force for interstitial hypertension in solid tumors: implications for vascular collapse. Cancer Res. 52, 5110–5114.

Butler, T.P., Grantham, F.H., Gullino, P.M., 1975. Bulk transfer of fluid in the interstitial compartment of mammary tumors. Cancer Res. 35, 3084–3088.

Chauhan, V.P., Stylianopoulos, T., Martin, J.D., Popović, Z., Chen, O., Kamoun, W.S., Bawendi, M.G., Fukumura, D., Jain, R.K., 2012. Normalization of tumour blood vessels improves the delivery of nanomedicines in a size-dependent manner. Nat. Nanotechnol. 7, 383–388.

Chernomordik, L.V., Kozlov, M.M., 2008. Mechanics of membrane fusion. Nat. Struct. Mol. Biol. 15, 675–683.

Clark, K., Vendt, B., Smith, K., Freymann, J., Kirby, J., Koppel, P., Moore, S., Phillips, S., Maffitt, D., Pringle, M., 2013. The Cancer Imaging Archive (TCIA): maintaining and operating a public information repository. J. Digit. Imaging 26, 1045–1057.

Connor, J., Yatvin, M.B., Huang, L., 1984. pH-sensitive liposomes: acid-induced liposome fusion. Proc. Natl. Acad. Sci. 81, 1715–1718.

Dalmark, M., Storm, H.H., 1981. A Fickian diffusion transport process with features of transport catalysis. Doxorubicin transport in human red blood cells. J. Gen. Physiol. 78, 349–364.

Danson, S.J., Middleton, M.R., 2001. Temozolomide: a novel oral alkylating agent. Expert Rev. Anticancer Ther. 1, 13–19.

Dewhirst, M.W., Secomb, T.W., 2017. Transport of drugs from blood vessels to tumour tissue. Nat. Rev. Cancer 17, 738–750.

Diez, B.D., Statkevich, P., Zhu, Y., Abutarif, M.A., Xuan, F., Kantesaria, B., Cutler, D., Cantillon, M., Schwarz, M., Pallotta, M.G., 2010. Evaluation of the exposure equivalence of oral versus intravenous temozolomide. Cancer Chemother. Pharmacol. 65, 727–734.

Eikenberry, S., 2009. A tumor cord model for doxorubicin delivery and dose optimization in solid tumors. Theor. Biol. Med. Modell. 6, 16–35.

El-Kareh, A.W., Secomb, T.W., 2000. A mathematical model for comparison of bolus injection, continuous infusion, and liposomal delivery of doxorubicin to tumor cells. Neoplasia 2, 325–338.

Friedman, H.S., Kerby, T., Calvert, H., 2000. Temozolomide and treatment of malignant glioma. Clin. Cancer Res. 6, 2585–2597.

Fung, L.K., Shin, M., Tyler, B., Brem, H., Saltzman, W.M., 1996. Chemotherapeutic drugs released from polymers: distribution of 1, 3-bis (2-chloroethyl)-l-nitrosourea in the rat brain. Pharm. Res. 13, 671–682.

Gao, J., Wang, Z., Liu, H., Wang, L., Huang, G., 2015. Liposome encapsulated of temozolomide for the treatment of glioma tumor: preparation, characterization and evaluation. Drug Discoveries Ther. 9, 205–212.

Garcion, E., Lamprecht, A., Heurtault, B., Paillard, A., Aubert-Pouessel, A., Denizot, B., Menei, P., Benoît, J.-P., 2006. A new generation of anticancer, drug-loaded, colloidal vectors reverses multidrug resistance in glioma and reduces tumor progression in rats. Mol. Cancer Ther. 5, 1710–1722.

Gasselhuber, A., Dreher, M.R., Partanen, A., Yarmolenko, P.S., Woods, D., Wood, B.J., Haemmerich, D., 2012. Targeted drug delivery by high intensity focused ultrasound mediated hyperthermia combined with temperature-sensitive liposomes: computational modelling and preliminary in vivo validation. Int. J. Hyperth. 28, 337–348.

Gasselhuber, A., Dreher, M.R., Rattay, F., Wood, B.J., Haemmerich, D., 2012. Comparison of conventional chemotherapy, stealth liposomes and temperature-sensitive liposomes in a mathematical model. PLoS ONE 7, e47453.

Goh, Y.-M.F., Kong, H.L., Wang, C.-H., 2001. Simulation of the delivery of doxorubicin to hepatoma. Pharm. Res. 18, 761–770.

Green, D.W., Perry, R.H. Perry's Chemical Engineers' Handbook/edición Don W. Green y Robert H. Perry, 1973.

Gross, J.F., Popel, A.S., 1979. Mathematical Models of Transport Phenomena in Normal and Neoplastic Tissue. CRC Press, Boca Raton, FL, USA.

Hanna, K.S., Mancini, R., Burtelow, M., Bridges, B., 2018. Aplastic anemia in a patient with anaplastic oligodendroglioma postradiation and concurrent temozolomide therapy: case report and review of the literature. J. Hematol. Oncol. Pharm. 8, 34–39.

Hatakeyama, H., Akita, H., Maruyama, K., Suhara, T., Harashima, H., 2004. Factors governing the in vivo tissue uptake of transferrin-coupled polyethylene glycol liposomes in vivo. Int. J. Pharm. 281, 25–33.

Huang, G., Zhang, N., Bi, X., Dou, M., 2008. Solid lipid nanoparticles of temozolomide: potential reduction of cardial and nephric toxicity. Int. J. Pharm. 355, 314–320.

Jain, R.K., 1987. Transport of molecules in the tumor interstitium: a review. Cancer Res. 47, 3039–3051.

Johnsen, K.B., Moos, T., 2016. Revisiting nanoparticle technology for blood–brain barrier transport: unfolding at the endothelial gate improves the fate of transferrin receptor-targeted liposomes. J. Control. Release 222, 32–46.

Kalyanasundaram, S., Calhoun, V., Leong, K., 1997. A finite element model for predicting the distribution of drugs delivered intracranially to the brain. Am. J. Physiol. 273, R1810–R1821.

Kanamala, M., Wilson, W.R., Yang, M., Palmer, B.D., Wu, Z., 2016. Mechanisms and biomaterials in pH-responsive tumour targeted drug delivery: a review. Biomaterials 85, 152–167.

Kimelberg, H., 2004. Water homeostasis in the brain: basic concepts. Neuroscience 129, 851–860.

Kulkarni, S.A., Feng, S.-S., 2011. Effects of surface modification on delivery efficiency of biodegradable nanoparticles across the blood–brain barrier. Nanomedicine 6, 377–394.

Kulkarni, V.S., Shaw, C., 2015. Essential Chemistry for Formulators of Semisolid and Liquid Dosages. Academic Press.

Kushner, B.H., Kramer, K., Modak, S., Cheung, N.-K.V., 2006. Irinotecan plus temozolomide for relapsed or refractory neuroblastoma. J. Clin. Oncol. 24, 5271–5276.

Lee, C.G., Fu, Y.C., Wang, C.H., 2005. Simulation of gentamicin delivery for the local treatment of osteomyelitis. Biotechnol. Bioeng. 91, 622–635.

Mangiola, A., Anile, C., Pompucci, A., Capone, G., Rigante, L., De Bonis, P., 2010. Glioblastoma therapy: going beyond Hercules Columns. Expert Rev. Neurother. 10, 507–514.

Maurer, N., Fenske, D.B., Cullis, P.R., 2001. Developments in liposomal drug delivery systems. Expert Opin. Biol. Ther. 1, 923–947.

Miller, C.R., Bondurant, B., McLean, S.D., McGovern, K.A., O'Brien, D.F., 1998. Liposome–cell interactions in vitro: effect of liposome surface charge on the binding and endocytosis of conventional and sterically stabilized liposomes. Biochemistry 37, 12875–12883.

Neeves, K., Lo, C., Foley, C., Saltzman, W., Olbricht, W., 2006. Fabrication and characterization of microfluidic probes for convection enhanced drug delivery. J. Control. Release 111, 252–262.

Newlands, E., Blackledge, G., Slack, J., Rustin, G., Smith, D., Stuart, N., Quarterman, C., Hoffman, R., Stevens, M., Brampton, M., 1992. Phase i trial of temozolomide (CCRG 81045: M&B 39831: NSC 362856). Br. J. Cancer 65, 287–291.

Newlands, E., Stevens, M., Wedge, S., Wheelhouse, R., Brock, C., 1997. Temozolomide: a review of its discovery, chemical properties, pre-clinical development and clinical trials. Cancer Treat. Rev. 23, 35–61.

Nhan, T., Burgess, A., Lilge, L., Hynynen, K., 2014. Modeling localized delivery of Doxorubicin to the brain following focused ultrasound enhanced blood-brain barrier permeability. Phys. Med. Biol. 59, 5987–6004.

Ostermann, S., Csajka, C., Buclin, T., Leyvraz, S., Lejeune, F., Decosterd, L.A., Stupp, R., 2004. Plasma and cerebrospinal fluid population pharmacokinetics of temozolomide in malignant glioma patients. Clin. Cancer Res. 10, 3728–3736.

Pineda, J., Jeitany, M., Andrieux, A., Junier, M., Chneiweiss, H., 2017. Intranasal administration of temozolomide delayed the development of brain tumors initiated by human glioma stem-like cell in nude mice. J. Cancer Sci. Ther. 9, 374–378.

Raghunathan, S., Evans, D., Sparks, J.L., 2010. Poroviscoelastic modeling of liver biomechanical response in unconfined compression. Ann. Biomed. Eng. 38, 1789–1800.

Ranganath, S.H., Fu, Y., Arifin, D.Y., Kee, I., Zheng, L., Lee, H.-S., Chow, P.K.-H., Wang, C.-H., 2010. The use of submicron/nanoscale PLGA implants to deliver paclitaxel with enhanced pharmacokinetics and therapeutic efficacy in intracranial glioblastoma in mice. Biomaterials 31, 5199–5207.

Rosso, L., Brock, C.S., Gallo, J.M., Saleem, A., Price, P.M., Turkheimer, F.E., Aboagye, E.O., 2009. A new model for prediction of drug distribution in tumor and normal tissues: pharmacokinetics of temozolomide in glioma patients. Cancer Res. 69, 120–127.

Saltzman, W.M., Radomsky, M.L., 1991. Drugs released from polymers: diffusion and elimination in brain tissue. Chem. Eng. Sci. 46, 2429–2444.

Schmidt, M.M., Wittrup, K.D., 2009. A modeling analysis of the effects of molecular size and binding affinity on tumor targeting. Mol. Cancer Ther. 8, 2861–2871.

Singh, R.P., Sharma, G., Kumari, L., Koch, B., Singh, S., Bharti, S., Rajinikanth, P.S., Pandey, B.L., Muthu, M.S., 2016. RGD-TPGS decorated theranostic liposomes for brain targeted delivery. Colloids Surf., B 147, 129–141.

Soltani, M., Chen, P., 2013. Numerical modeling of interstitial fluid flow coupled with blood flow through a remodeled solid tumor microvascular network. PLoS ONE 8, e67025.

Swabb, E.A., Wei, J., Gullino, P.M., 1974. Diffusion and convection in normal and neoplastic tissues. Cancer Res. 34, 2814–2822.

Tagami, T., Ernsting, M.J., Li, S.-D., 2011. Optimization of a novel and improved thermosensitive liposome formulated with DPPC and a Brij surfactant using a robust in vitro system. J. Control. Release 154, 290–297.

Tagami, T., May, J.P., Ernsting, M.J., Li, S.-D., 2012. A thermosensitive liposome prepared with a Cu 2+ gradient demonstrates improved pharmacokinetics, drug delivery and antitumor efficacy. J. Control. Release 161, 142–149.

Tan, W.H.K., Lee, T., Wang, C.-H., 2003. Delivery of etanidazole to brain tumor from PLGA wafers: a double burst release. System 82, 278–288.

Tzafriri, A.R., Lerner, E.I., Flashner-Barak, M., Hinchcliffe, M., Ratner, E., Parnas, H., 2005. Mathematical modeling and optimization of drug delivery from intratumorally injected microspheres. Clin. Cancer Res. 11, 826–834.

Vertut-Doï, A., Ishiwata, H., Miyajima, K., 1996. Binding and uptake of liposomes containing a poly (ethylene glycol) derivative of cholesterol (stealth liposomes) by the macrophage cell line J774: influence of PEG content and its molecular weight. Biochim. Biophys. Acta (BBA)-Biomembranes 1278, 19–28.

Wang, C.-H., Li, J., Teo, C.S., Lee, T., 1999. The delivery of BCNU to brain tumors. J. Control. Release 61, 21–41.

Weller, R.O., Djuanda, E., Yow, H.-Y., Carare, R.O., 2009. Lymphatic drainage of the brain and the pathophysiology of neurological disease. Acta Neuropathol. 117, 1–14.

Wu, N.Z., Da, D., Rudoll, T.L., Needham, D., Whorton, A.R., Dewhirst, M.W., 1993. Increased microvascular permeability contributes to preferential accumulation of Stealth liposomes in tumor tissue. Cancer Res. 53, 3765–3770.

Xue, J., Zhao, Z., Zhang, L., Xue, L., Shen, S., Wen, Y., Wei, Z., Wang, L., Kong, L., Sun, H., 2017. Neutrophil-mediated anticancer drug delivery for suppression of postoperative malignant glioma recurrence. Nat. Nanotechnol. 12, 692–700.

Yang, B., Li, X., He, L., Zhu, Y., 2018. Computer-aided design of temozolomide derivatives based on alkylglycerone phosphate synthase structure with isothiocyanate and their pharmacokinetic/toxicity prediction and anti-tumor activity in vitro. Biomed. Rep. 8, 235–240.

Zhan, W., Gedroyc, W., Yun Xu, X., 2014. Mathematical modelling of drug transport and uptake in a realistic model of solid tumour. Protein Peptide Lett 21, 1146–1156.

Zhan, W., Wang, C.-H., 2018. Convection enhanced delivery of liposome encapsulated doxorubicin for brain tumour therapy. J. Control. Release 285, 212–229.

Zhan, W., Wang, C.-H., 2018. Convection enhanced delivery of chemotherapeutic drugs into brain tumour. J. Control. Release 271, 74–87.

Zhan, W., Xu, X.Y., 2013. A mathematical model for thermosensitive liposomal delivery of Doxorubicin to solid tumour. J. Drug Delivery 2013, 172529.

Zhang, A., Mi, X., Xu, L.X., 2008. Study of Thermally Targeted Nano-Particle Drug Delivery for Tumor Therapy, ASME 2008 First International Conference on Micro/

Nanoscale Heat Transfer. American Society of Mechanical Engineers, pp. 1399–1406.

Zhao, J., Salmon, H., Sarntinoranont, M., 2007. Effect of heterogeneous vasculature on interstitial transport within a solid tumor. Microvasc. Res. 73, 224–236.

Ziemys, A., Klemm, S., Milosevic, M., Yokoi, K., Ferrari, M., Kojic, M., 2016. Computational analysis of drug transport in tumor microenvironment as a critical compartment for nanotherapeutic pharmacokinetics. Drug Delivery 23, 2524–2531.